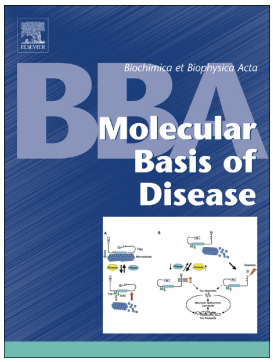

Functional characterization of MODY2 mutations in the nuclear export signal of glucokinase

Angel Gutierrez-Nogués, Carmen-María García-Herrero, Josep Oriola, Olivier Vincent, María-Angeles Navas

PII: S0925-4439(18)30160-1
DOI: doi:10.1016/j.bbadis.2018.04.020
Reference: BBADIS 65117

To appear in:

Received date: 25 January 2018
Revised date: 23 March 2018
Accepted date: 23 April 2018

Please cite this article as: Angel Gutierrez-Nogués, Carmen-María García-Herrero, Josep Oriola, Olivier Vincent, María-Angeles Navas , Functional characterization of MODY2 mutations in the nuclear export signal of glucokinase. The address for the corresponding author was captured as affiliation for all authors. Please check if appropriate. Bbadis(2018), doi:10.1016/j.bbadis.2018.04.020

Functional characterization of MODY2 mutations in the Nuclear Export Signal of Glucokinase.

Angel Gutierrez-Nogués[a], Carmen-María García-Herrero[a], Josep Oriola[b], Olivier Vincent[c], and María-Angeles Navas[a,d,e]

a. Departamento de Bioquímica y Biología Molecular III. Facultad de Medicina, Universidad Complutense de Madrid and Instituto de Investigación Sanitaria del Hospital Clínico San Carlos. Madrid, Spain.
b. Servicio de Bioquímica y Genética Molecular. Hospital Clínic. Departamento de Ciencias Fisiológicas I. Facultad de Medicina. Universidad de Barcelona, Spain.
c. Instituto de Investigaciones Biomédicas Alberto Sols. Consejo Superior de Investigaciones Científicas-Universidad Autónoma de Madrid. Madrid, Spain.
d. Centro de Investigación Biomédica en Red de Diabetes y Enfermedades Metabólicas (CIBERDEM), www.ciberdem.net, Instituto de Salud Carlos III. Madrid, Spain.
e. Instituto de Investigación Sanitaria del Hospital Clínico San Carlos (IdISSC). Madrid, Spain

Corresponding author**:** María-Angeles Navas. Departamento de Bioquímica y Biología Molecular III. Facultad de Medicina, Universidad Complutense de Madrid. Madrid, Spain. Phone: +34913941449; FAX: +34913941691. E-mail: manavas@med.ucm.es

ABSTRACT

Glucokinase (GCK) plays a key role in glucose homeostasis. Heterozygous inactivating mutations in the *GCK* gene cause the familial, mild fasting hyperglycaemia named MODY2. Besides its particular kinetic characteristics, glucokinase is regulated by subcellular compartmentation in hepatocytes. Glucokinase regulatory protein (GKRP) binds to GCK, leading to enzyme inhibition and import into the nucleus at fasting. When glucose concentration increases, GCK-GKRP dissociates and GCK is exported to the cytosol due to a nuclear export signal (NES). With the aim to characterize the GCK-NES, we have functionally analysed nine MODY2 mutations located within the NES sequence.

Recombinant GCK mutants showed reduced catalytic activity and, in most cases, protein instability. Most of the mutants interact normally with GKRP, although mutations L306R and L309P impair GCK nuclear import in cotransfected cells. We demonstrated that GCK-NES function depends on exportin 1. We further showed that none of the mutations fully inactivate the NES, with the exception of mutation L304P, which likely destabilizes its α-helicoidal structure. Finally, we found that residue Glu300 negatively modulates the NES activity, whereas other residues have the opposite effect, thus suggesting that some of the NES spacer residues contribute to the low affinity of the NES for exportin 1, which is required for its proper functioning.

In conclusion, our results have provided functional and structural insights regarding the GCK-NES and contributed to a better knowledge of the molecular mechanisms involved in the nucleo-cytoplasmic shuttling of glucokinase. Impairment of this regulatory mechanism by some MODY2 mutations might contribute to the hyperglycaemia in the patients.

Key Words:

MODY, glucokinase, glucokinase mutation, glucokinase regulatory protein, nuclear export signal.

Abbreviations:

CRM1	Chromosome Region Maintenance 1
F1P	Fructose 1-phosphate
F6P	Fructose 6-phosphate
GCK	glucokinase
GFP	green fluorescent protein
GKRP	glucokinase regulatory protein
GST	glutathione S-transferase
HA	hemagglutinin
NES	Nuclear export signal
RAI	relative activity index
WT	wild type

1. INTRODUCTION

Glucokinase (GCK) plays a central role in the regulation of glucose metabolism. Its activity is restricted to cells with important roles in whole-body glucose homeostasis [1]. In pancreatic beta-cells GCK acts as glucose sensor by integrating blood glucose levels and glucose metabolism with insulin secretion. In hepatocytes, where glucokinase is also expressed, its activity controls glycogen accumulation, glycolysis and gluconeogenesis rates. Moreover, a role of glucokinase has also been reported in the brain, pancreatic alpha cells and pituitary gonadotropes, for review see [2]. *GCK* mutations can result in monogenic disorders characterized by hyper or hypoglycaemia. Heterozygous activating mutations cause hyperinsulinemic hypoglycaemia. Homozygous inactivating mutations cause permanent neonatal diabetes mellitus, whereas heterozygous inactivating mutations cause maturity-onset diabetes of the young type 2 (MODY2) [3]. The patophysiological mechanism of GCK associated disorders is a defect in glucose sensing that results in modification of the glucose threshold for beta-cell insulin secretion. Additionally, defects in liver glycogen storage and increased rate of gluconeogenesis have been demonstrated in MODY2 patients [4,5].

Glucokinase belongs to the hexokinase family (GCK is also named hexokinase IV), which converts glucose in glucose-6-phosphate with ATP as second substrate. This reaction is the first limiting step of glucose utilization in hepatocytes and beta-cells. The function of glucokinase is based on its particular kinetic characteristics, mainly low affinity and cooperativity for glucose. These properties are conferred by multiple conformational protein structure states. Briefly, in the absence of glucose, GCK has an inactive super-open conformation. Conversely, the glucose-bound enzyme adopts an active closed conformation [6,7]. In addition, glucokinase can be regulated by tissue-specific posttranscriptional mechanisms [2]. In the liver, glucokinase is also regulated through protein-protein interactions by the glucokinase regulatory protein (GKRP), which inhibits the enzyme and also induces its nuclear retention in hepatocytes [8,9]. GCK-GKRP interaction is strengthened by fructose-6-phosphate (F6P) and counteracted by fructose-1-phosphate (F1P), which bind to the same site of GKRP [10,11]. During fasting, at low glucose concentrations, GKRP-F6P anchors the super-open GCK form, allowing its import into the nucleus. Mutational and structural studies of GKRP-bound GCK have shown that the GKRP-binding surface is located at the allosteric site in the hinge region of GCK, which is exposed in the super-open conformation [11-15]. Upon binding to GKRP, GCK translocates to the nucleus in hepatocytes or in heterologous cells co-transfected with GKRP and GCK, and the absence of GKRP results in exclusive cytoplasmic locatization of this enzyme [9,16,17]. After feeding, when glucose (and fructose) concentrations rise, GCK adopts an

active glucose-bound closed conformation and dissociates from GKRP-F1P. Substrate binding causes a structural rearrangement of GCK, which results in the dissociation of the complex [15]. The dissociation of GCK from GKRP occurs prior to being exported from the nucleus to the cytoplasm [18,19]. The enzyme nuclear export is mediated by a leucine-rich nuclear export signal (NES) covering aminoacids 300 to 310 of glucokinase (GCK-NES: ^{300}ELVRLVLLKLV^{310}) [17].
Due to the central role of glucokinase in the regulation of glucose homeostasis, this enzyme has been considered as a potential target for the development of new anti-diabetic drugs. However, tackling such a challenge requires a thorough knowledge of GCK regulatory mechanisms [20,21]. The biochemical characterization of *GCK* mutations associated to glycemic disorders has contributed significant insights into the regulatory mechanism of this enzyme [3]. In this work, we carried out a systematic analysis of MODY2 mutations within the GCK-NES sequence.

2. MATERIAL AND METHODS

2.1. Selection of MODY2 mutations in the Nuclear Export Signal of glucokinase.

We selected a series of GCK mutations covering the NES sequence of this enzyme. Mutations E300Q, E300K, R303W, L304P, L306R, R308W, L309H and L309P had been previously identified [22-25, 3]. Mutation V302E is a novel mutation identified in this work.

2.2. Subjects and genetic analysis.

The patient bearing V302E mutation was referred to our laboratory at the Hospital Clinic of Barcelona for a molecular diagnosis of MODY. A 27 years old woman of caucasian descent, presented repetitive mild fasting hyperglycaemia. A 75-g OGTT resulted in blood glucose concentrations of 6.1, 9.3 and 6.4 mmol/l and insulin of 7.18, 18.5, 22.9 and 20.2 mU/l at 0, 60 and 120 min respectively. Her 6 years old daughter and 4 years old son also presented repetitive mild fasting hyperglycaemias. Body mass index was 21.5, 19.5 and 16 kg/m^2 for the patient, her daughter and son, respectively. Informed consent was obtained from the subject or their parents. The study was performed according to the Declaration of Helsinki as revised in 2008 and approved by the local ethical committee. *GCK* genetic analysis was performed as described in [26].

2.3. Plasmid constructs and mutagenesis.

Plasmid pGEX-5X.2-GCK express human wild type beta-cell GCK fused to glutathione-S-transferase (GST-GCK) [27]. Plasmid p-FLAG-ctc-hGKRP-FlagC contains human Flag-tagged GKRP [28]. Plasmid pEGFP-N2-ratGCK(299-359) express rat GCK residues 299 to 359 as an N-terminal enhanced green fluorescent protein (GFP) fusion protein ($GCK^{(299-359)}$-GFP) [17]. Plasmid pYFP-CRM1 contains the human cDNA for CRM1 (Chromosome Region Maintenance 1)/exportin1 [29]. Plasmids pEGFP-C3-GCK (expressing human β-cell GCK as a C-terminal GFP fusion protein GFP-GCK), pGKRP-mCherry (expressing the human GKRP as an N-terminal mCherry fusion protein (GKRP-mCherry), pmCherry and pCMV-HA-CRM1 (expressing hemagglutinin (HA) tagged-exportin1) were prepared as described in Supplementary Material and Methods. Mutagenesis was performed as previously described [30] by using primers shown on Supplementary Table S1.

2.4. Protein production and purification.

Recombinant wild-type and mutant GST-GCK were bacterially expressed, purified and stored as described previously [27]. Flag tagged human GKRP was purified from *E. coli* as in [28] with the modifications detailed in Supplementary Material and Methods.

2.5. GCK enzymatic assays and in silico structural analysis.

Determination of kinetic parameters, thermal inactivation, inhibition by GKRP and structural analysis were performed as previously described [25,27,30]. See Supplementary Material and Methods.

2.6. Cell culture, transient transfection and treatment with leptomycin B.

HEK293T cells were a gift from Dr. C. Hernández-Sánchez (Centro de Investigaciones Biológicas, Madrid, Spain) and were cultured in DMEM containing glucose 25 mmol/l. HepG2 cells were purchased from the American Type Culture Collection (ATCC HB-8065, Manassas, VA, USA) and cultured in MEM containing glucose 5.5 mmol/l. See Supplementary Material and Methods. Transient transfections of HEK293T were performed with lipofectamine (Invitrogen, Carlsbad, CA,

USA) and HepG2 with XtremeGENE HP (Roche Diagnostics, Mannheim, Germany) according to the manufacturer's instructions, see Supplementary Material and Methods. When indicated, cells were incubated for 6 h with 40 nmol/l of leptomycin B (Sigma-Aldrich, St Louis, MO, USA).

2.7. Western blot analysis

Western blot analysis was performed in transfected cells to detect GFP, mCherry and actin as detailed in Supplementary Material and Methods.

2.8. Inmunocytochemistry, fluorescence microscopy and image analysis.

Cells, cultured and transfected on coverslips (Menzel-Gläser,Braunschweig, Germany), were fixed with 4% formaldehyde (Merck Sharp & Dohme International, Whitehouse Station, NJ, USA) 42 h after transfection. Following nuclei staining with 4',6-diamidino-2-phenylindole (DAPI, Invitrogen), coverslips were mounted with *Fluoromount G* (Electron Microscopy Sciences, Hatfield, PA, USA). For inmunocytochemistry, fixed cells were permeabilised with 0.4% Triton X-100 and blocked in 10% normal goat serum (Sigma-Aldrich) with 0.1% Triton X100 in PBS. Cells were incubated 2 h with *Monoclonal Rat anti-HA Tag antibody* (1:100; Roche), washed with blocking buffer and then incubated for 1 h with goat anti rat IgG (H&L): TexasRed (1:200; AbD serotec, Oxford, UK). The analysis of fluorescent proteins was performed with an epifluorescence microscope Leica DMRB (Leica Microsystems, Wetzlar, Germany) or with a laser confocal microscope Leica SP2 AOBS. Excitations wavelengths of 405 nm, 488 nm and 543 nm were used for detection of DAPI, GFP and Texas-Red/mCherry, respectively. For each experimental condition, at least 290 cells were visually analyzed for the intracellular distribution of the fluorescence signal with the Leica DMRB fluorescence microscope with an HC PLAN APO 20x/0.70 objective. Fluorescence distribution in individual cells was classified by visual inspection as homogeneous, nuclear, cytoplasmic or perinuclear. See Supplementary Material and Methods for further details. Fluorescent images were captured using the confocal system with an HCX PL APO 63x/1.4-0.6 Oil Lbd BL objective lens. Confocal images were processed and fluorescence intensities of images were quantified with the ImageJ 1.48v software (National Institutes of Health, Bethesda, USA). At least 10 cells were analyzed for each experimental condition. Equal areas of cytoplasm and nucleus were measured for each cell image. The nuclear/cytoplasmic fluorescence intensity ratio (N/C) was calculated by dividing the nuclear intensity by the cytoplasmic intensity.

2.9. Yeast two-hybrid analysis.

Two-hybrid studies were performed as described previously [27]. Plasmid encoding human GKRP fusion protein to the Gal4 Binding Domain (GBD) was constructed as described in [26]. Plasmids encoding human GCK fusion proteins to the Gal4 Activation Domain (GAD) were prepared as described in Supplementary Material and Methods.

2.10. Statistical analysis.

Results are shown as means ± SD, and statistical significance was analysed by the two-tailed Student's *t* test. *p* values of <0.05 were considered statistically significant.

3. RESULTS

3.1.Identification of a novel MODY2 mutation within the GCK-NES.

Sequencing of beta-cell *GCK* gene in the diabetic patient and her daughter and son revealed a heterozygous change in exon 8, c.905T>A, which results in novel mutation V302E. This mutation has neither been found in 1000 Caucasian individuals nor in the Exome Aggregation Consortium (ExAC) database.

3.2. Effects of GCK-NES mutations on glucokinase activity.

3.2.1 Enzymatic characterization.

Kinetic analysis was performed with recombinant GST-GCK, the V302E mutant derivative and other known MODY2 mutants within the GCK-NES, for which kinetic constants were not reported yet: L304P, L306R and L309H. Results are shown in Table 1. Purification yield was lower for proteins carrying mutations V302E, L304P or L306R, and glucokinase activity of all the mutants was reduced by at least 83% (RAI ≤ 0.17), the strongest effect being caused by L306R (RAI = 0.03). The lower activity of these mutants was mainly due to a reduced catalytic constant (Kcat) value. Additionally, all the mutations produced a slight but significant negative effect on the affinity

for glucose ($S_{0.5}$ values are 29 to 48 % higher). The affinity for ATP (Km) was also slightly affected.

3.2.2 Thermolability of mutants.

The activity of GST-GCK and mutant derivatives V302E, L304P and L309H was measured at different temperatures to analyse whether these mutations affect GCK protein stability. Mutant GST-GCK(L306R) was excluded from this assay since its activity was too low to obtain accurate results (Table 1). Figure 1 shows that mutation L309H did not significantly affect GCK activity when incubated at temperatures up to 50ºC. In contrast, mutations V302E and L304P increased temperature-dependent enzyme inactivation (Fig. 1a and b). Mutation L304P produced the strongest effect since GST-GCK(L304P) showed significant inactivation at temperatures above 37 ºC (Fig. 1a).

3.2.3. Effect of mutations on GCK enzymatic inhibition by GKRP.

To assess whether these mutations alter the inhibition of GCK by its regulatory protein GKRP, the activity of GST-GCK mutants was assayed in the presence of increasing concentrations of purified recombinant human GKRP. The activity of mutants was compared to both wild type GST-GCK and GST-GCK(A456V), which was previously described to be largely insensitive to GKRP inhibition [13]. Mutants L306R and L309P were excluded from this assay because of their low specific activities (Table 1 and [31]). Figure 2 shows that none of the GCK-NES mutations affect the inhibition by GKRP.

3.3. *Effects of mutations on glucokinase subcellular localization*

3.3.1. Effects of mutations on GKRP-dependent GCK nuclear import.

In hepatocytes, nuclear import of GCK depends on GKRP binding, while nuclear export depends on GCK-NES activity. We first analysed whether GKRP-dependent nuclear import of GCK was altered by these mutations. HepG2 cells were transiently co-transfected with GFP-tagged human wild-type or mutant GCK and mCherry-tagged GKRP fusion plasmids and analysed by fluorescence microscopy. We found that the nuclear translocation of GCK is fully dependent on GKRP. Localization of GFP-GCK is cytosolic in the absence of co-transfected GKRP-mCherry (Fig. 3) and the same result is observed with all the mutants (not shown). As expected, co-expression of GKRP-mCherry results in the nuclear translocation of wild type GFP-GCK and most

of the mutants, except the mutants L306R and L309P which were retained in the cytoplasm (Fig. 3). Co-expression of these two mutants and GKRP-mCherry was confirmed by immunoblotting (Supplementary Fig. S1a). Interestingly, GKRP-mCherry was predominantly nuclear in all cases, except in some cells co-expressing GFP-GCK(L309P), where both GCK and GKRP fusions were detected in the cytosol (Fig. 3 and Supplementary Table S2).

3.3.2. Two hybrids assays to test the physical interaction between GCK mutants and GKRP.

To investigate whether mutations L306R and L309P impair the physical interaction of GCK with GKRP, we analysed these two mutants as well as others in yeast two-hybrid assays (Fig. 4). In agreement with the GKRP inhibition assays (Fig. 2), most of the mutants were able to bind GKRP (Fig. 4). In contrast, and as expected from the localization studies, mutant GCK(L306R) did not interact with the regulatory protein. Unexpectedly, mutant GCK(L309P) binds to GKRP although this interaction does not appear to be sufficient to trigger the nuclear translocation of glucokinase.

3.3.3. Effects of GCK mutations on the NES function.

Next we aimed to determine whether these MODY2 mutations affect the GCK-NES activity. We used a previously described GFP-fusion protein containing rat GCK amino acids 299 to 359 ($GCK^{(299-359)}$-GFP, Fig. 5) because this construct can diffuse into the nucleus independently of GKRP [17]. Expression of wild type and mutant $GCK^{(299-359)}$-GFP fusion proteins in HEK293T cells was confirmed by immunoblotting (Supplementary Fig. S1b) and subcellular localization of GFP fusions was assessed by fluorescence microscopy. As shown in Fig. 6, unfused GFP was slightly enriched in the nucleus (N/C= 1.4 ±0.2) in most cells (65 ±6 %). In agreement with previous work [17], the presence of the NES in wild type $GCK^{(299-359)}$-GFP prevents GFP nuclear enrichment. This effect was visualised by confocal microscopy as a partial enrichment of the GFP-fusion protein in the cytoplasm (N/C= 0.75 ±0.08; Fig 6). This partial cytoplasmic enrichment was not detectable by epifluorescence microscopy and the effect of the NES was only visualised as a shift from the slight nuclear enrichment to a homogeneous distribution of GFP fluorescence in most cells (Supplementary Table S3). In contrast, and as unfused GFP, the mt3 control inactive-NES mutant was slightly enriched in the nucleus of most cells (78 ±5 %; N/C= 1.61 ±0.35; Fig. 6).

We then analysed the nuclear enrichment of mutant $GCK^{(299-359)}$-GFP fusion proteins to evaluate the exporting activity of the mutated NES sequences (Fig 6). Mutation K308W (note that K308W in the rat sequence corresponds to human MODY2 mutation R308W, Fig. 5) did not change the percentage of cells with nuclear enrichment of the GFP fusion protein (25 ±3 %; Fig 6). However,

we found that more than 50% of cells (53 ±2 %) accumulated fluorescence surrounding the nucleus (Fig. 6). Such perinuclear distribution was more pronounced in Cos7 cells (Supplementary Fig. S2). Strikingly, mutations E300K and E300Q increased the strength of the NES since more than 95% of transfected cells accumulated the GFP fusion protein in the cytoplasm (N/C= 0.51 ±0.03 and 0.55 ±0.1, respectively; Fig. 6, compare WT and E300K or E300Q). In contrast, mutations at positions 302, 303, 304 and 309 impaired the NES function, with effects ranging from mild (mutations L309P and L309H; N/C= 0.99 ±0.14 and 0.99 ±0.1, respectively; Fig. 6) to moderate and severe (V302E, R303W and L304P; N/C= 1.36 ±0.24, 1.35 ±0.13 and 1.63 ±0.18, respectively; Fig. 6). The opposite effect of E300K and L304P on NES activity was further analysed by introducing both mutations into the GCK$^{(299-359)}$-GFP fusion protein. Double mutant GCK$^{(299-359)}$(E300K/L304P)-GFP was predominantly nuclear (N/C= 1.39 ±0.13; Fig. 6), thus indicating that the stronger NES activity of the E300K mutant is fully suppressed by the L304P mutation (Fig. 6, compare E300K with E300K/L304P).

To determine whether the GCK-NES is recognized by the major exportin, CRM1/exportin1, we analysed the nuclear/cytoplasmic distribution of GCK$^{(299-359)}$-GFP fusion proteins in HEK293T transfected cells in conditions where exportin activity was either inhibited by leptomycin B or increased by CRM1 overexpression. As shown in Supplementary Fig. S3, leptomycin B inhibits the NES activity of both wild type and mutant GCK$^{(299-359)}$-GFP fusion proteins, which accumulate in the nucleus (N/C= 1.45 ±0.3) in most cells (70 ±7 %). Moreover, the percentage of GCK$^{(299-359)}$(K308W)-GFP transfected cells with perinuclear fluorescence was reduced to 30 ±4 % (Supplementary Table 4). To investigate the effects of CRM1 overexpression, HEK293T cells were co-transfected with GCK$^{(299-359)}$-GFP fusion proteins plus HA-tagged CRM1. Co-transfected cells were analysed by GFP fluorescence and HA-Texas-Red immunofluorescent staining (Fig 7). As expected, unfused GFP was mostly nuclear and thus insensitive to CRM1. In contrast, CRM1 overexpression resulted in a predominant cytoplasmic localization of GCK$^{(299-359)}$-GFP (N/C= 0.53 ±0.11; Fig. 7). Overexpressed HA-CRM1 efficiently exported most of the mutant GFP fusion proteins at the same extent as the wild type (Fig 7). However, about a 30% of co-transfected cells expressing the L304P mutant, alone or combined with E300K, were insensitive to CRM1 overexpression and accumulated the GFP-fusion in the nucleus (N/C= 1.25 ±0.22 and 1.2 ±0.15, respectively). The same effect was observed with the inactive-NES mt3 control mutant (N/C = 1 ±0.17; Fig 7). Overexpression of CRM1 did not substantially change the percentage of cells with perinuclear accumulation of GCK$^{(299-359)}$(K308W)-GFP (42 ±3%).

4. DISCUSION

Functional characterization of naturally occurring GCK mutations in patients with impaired glucose homeostasis has widened our knowledge of the catalytic and regulatory mechanisms of this enzyme [3]. In this work, we have biochemically characterized a group of GCK-MODY mutations within the α8-helix containing a nuclear export signal. α8-helix is found on the surface of the large domain of glucokinase, distant from the deep cleft that hosts the active site [6] (Fig. 8). We would predict that mutations V302E, L304P, L306R and L309H cause structural changes in the α8-helix by introducing polar residues in a hydrophobic environment and because of steric conflicts with neighbouring residues (Fig. 8). Indeed, we found that mutations V302E, L304P, L306R and L309H inactivate GST-GCK enzymatic activity by reducing strongly Kcat values and slightly glucose affinity, and likely decreasing protein stability, as suggested by the thermal inactivation and reduced purification yield of most of the recombinant mutant proteins *in vitro*. These findings are consistent with previous results showing that mutation L304P induced faster GCK-protein degradation in MIN6 cells [32]. Moreover, mutations E300Q, E300K, R303W, R308W and L309P have also been shown to decrease protein stability [25,33-37]. Taken together, these data indicate that α8-helix is important for glucokinase stability and kinetics.

Transport of proteins larger than the exclusion limit size (≈ 40 kDa) through the nuclear pore is mediated by importins and exportins, which recognize nuclear localization signals (NLS) and NES, respectively, in the cargo protein [38]. Although a GCK NLS has been recently reported to be functional in pancreatic beta-cells, GCK nuclear import in hepatocytes depends on its interaction with GKRP [39,17]. Previous analysis of the crystal structure of the GCK-GKRP complex indicates that GCK α8-helix is not directly involved in the interaction with GKRP [15] [11] (Fig. 8c). Accordingly, we found that most of the GCK mutants analysed here are inhibited *in vitro* by recombinant human GKRP, do interact with the regulatory protein in the yeast two–hybrid system and are translocated to the nucleus when co-expressed with GKRP in cultured cells. Exceptions are GCK mutants L306R and L309P, which are not detected in the cell nucleus even when GKRP was overexpressed. Consistently, mutation L306R prevents GCK binding to GKRP in yeast two-hybrid. Similar results have been reported for GCK mutant L309R [40]. Substitutions of hydrophobic leucine residues by basic arginine in the α8-helix may induce GCK folding defects, thus preventing recognition by GKRP. Surprisingly, mutant L309P still interacts with the regulatory protein in yeast two-hybrid. We found that leptomycin B does not induce the nuclear

accumulation of GFP-GCK(L309P) (results not shown) and that mutation L309P does not activate the GCK-NES, ruling out the possibility of a more active nuclear export resulting in the cytoplasmic accumulation of this mutant. We found that some HepG2 cells expressing GFP-GCK(L309P) retain GKRP-mCherry in the cytoplasm, thus supporting the idea that these two proteins interact but cannot be imported to the nucleus. One possible explanation is that mutation L309P impairs the conformational adjustment of the GCK-GKRP dimer [41] or that the mutant GCK-GKRP complex is not recognized by the import machinery.

Glucokinase contains a functional NES (^{300}ELVRLVLLKLV^{310}) that fits the NES consensus class 1b for the major export receptor exportin1/CRM1 (ϕ1-X2-ϕ2-X2-ϕ3-X-ϕ4, where ϕ is a hydrophobic residue, mainly Leu, but also Ile, Val, Phe or Met, and X might be any aminoacid) [17,42,43]. GKRP is required for GCK nuclear import but not for its nuclear export [17,18]. Since some of the mutations in GCK α8-helix impair its nuclear import, we used a previously developed method [17] to analyse the specific effect of these mutations on GCK-NES activity. This approach uses a small GFP-fusion protein (34 kDa) containing residues 299-359 of rat glucokinase, which can diffuse freely both into and out of the nucleus and thus does not require GKRP-dependent import. In agreement with previous work [17], we found that GCK-NES (residues 300 to 310) mediates nuclear export in our cultured cells and that NES activity is impaired in the mt3 control mutant. We further demonstrated that GCK-NES function requires exportin1/CRM1 by showing that nuclear export of the GFP-fusion protein is inhibited by leptomycin B and enhanced upon CRM1 overexpression. CRM1-interacting NES are diverse but share common characteristics such as a low affinity for CRM1 and hydrophobic residues that bind a hydrophobic groove in CRM1 [42,44,45]. Our mutational analysis has uncovered some functional and structural features of the GCK-NES. The MODY2 mutations L304P, L309H and L309P affect hydrophobic residues ϕ2 and ϕ4, while mutations E300K, E300Q, V302E, R303W and K308W (rat K308W corresponds to human R308W mutation) affect spacer positions. Once bound to CRM1, many NESs adopt an amphipathic α-helix conformation at the N-terminus (ϕ1-ϕ3), and have a more relaxed structure at the C-terminus (ϕ3-ϕ4) [44,45]. This may explain why proline substitution at ϕ2 position has a stronger inhibitory effect than at ϕ4. Indeed, mutations L309P produces just a slight decrease in export activity, whereas mutation L304P strongly inactivates the NES. Spacer residues are also important for NES activity [44,46]. For instance, bulky tryptophan residues are rarely found at the C-termini of NES [46]. The substitutions of basic residues to tryptophan in R303W and K308W mutants produce different effects. The R303W substitution between ϕ1 and ϕ2 disturbs the N-terminal amphipathic helix and, as expected, results in a weaker NES. In contrast, the K308W

substitution between ϕ3 and ϕ4 induces a perinuclear distribution of the GFP fusion protein. Interestingly, substitution at the same position in a synthetic NES has been shown to produce the same localization pattern [47]. Such NES, referred as supraphysiological, strongly interacts with CRM1 and impair nuclear export by blocking export complexes at nuclear pores. Previous work reported that acidic residues are found at relative high frequency at spacer positions and that substitution of neutral residues flanking ϕ1 to glutamate enhance CRM1 binding [48,46,44]. However, the negative effect of mutation V302E on export activity and the positive effect of mutations E300K and E300Q rather suggests that the presence of Glu next to ϕ1 weakens GCK-NES activity. We hypothesize that Glu300 contributes to the low affinity of the NES for CRM1, which is required for its proper functioning. In summary, our results support the idea that spacer residues of the GCK-NES modulate its activity either negatively or positively, thereby contributing to the fine-tuning of its function.

The effect of GCK-NES mutations on enzyme kinetics and protein stability might account for the hyperglycaemia that characterizes MODY2 patients, since reduced GCK activity would increase the threshold for glucose stimulated insulin release in beta-cells [31,37,49]. However, a more in depth functional characterization of these MODY2 mutations has allowed uncovering defects at other levels of GCK regulation, such as its subcellular localization. Translocation of GCK between cytoplasm and nucleus in hepatocytes depends on its interaction with GKRP, which is modulated by nutrients (mainly glucose and fructose). During periods of hypoglycaemia, GKRP inhibits and sequesters GCK in the nucleus and this glucokinase pool can be rapidly mobilized in response to increased cellular glucose [8,19]. Our results indicate that some of the MODY2 mutations in the GCK-NES likely impair the nucleo-cytoplasmic shuttling of GCK in the liver. Taking into account the important role of the liver in the homeostasis of blood glucose, this additional defect might contribute to the hyperglycaemia in these patients.

Hepatoselective glucokinase activators have been identified in the last years with the aim of developing new treatments for type II diabetes [50]. Some of these compounds act as GCK-GKRP disruptors that promote GCK translocation from the nucleus to the cytoplasm [51,52]. In this context, our findings contribute to a better knowledge of the molecular mechanisms involved in the nucleocytoplasmic shuttling of glucokinase.

Acknowledgements

We thank Mark Magnuson (Vanderbilt University, USA) for providing plasmids pEGFP-N2-ratGCK(299-359) wild type and mt3 mutant, Katy Brocklehurst (AstraZeneca, UK) for providing plasmid p-FLAG-ctc-hGKRP-FlagC and Carmen Rivas (Centro Nacional de Biotecnología, Spain) for providing plasmid pYFP-CRM1.

Funding

This work was supported by the Instituto de Salud Carlos III grant PI100424.

Duality of interest

The authors are not aware of any duality of interest.

Contribution statement

AGN contributed to the study design, researched and analysed data and revised the intellectual content of the manuscript. CMGH and JO researched and analysed data and revised the intellectual content of the manuscript. OV researched and analysed data and reviewed and edited the manuscript. MAN designed the study, analysed data and wrote the manuscript. All authors approved the final version of the manuscript.

References

[1] F.M. Matschinsky, M.A. Magnuson, D. Zelent, T.L. Jetton, N. Doliba, Y. Han, R. Taub, J. Grimsby, The network of glucokinase-expressing cells in glucose homeostasis and the potential of glucokinase activators for diabetes therapy, Diabetes, 55 (2006) 1-12.
[2] F.M. Matschinsky, Assessing the potential of glucokinase activators in diabetes therapy, Nat Rev Drug Discov, 8 (2009) 399-416.
[3] K.K. Osbak, K. Colclough, C. Saint-Martin, N.L. Beer, C. Bellanne-Chantelot, S. Ellard, A.L. Gloyn, Update on mutations in glucokinase (GCK), which cause maturity-onset diabetes of the young, permanent neonatal diabetes, and hyperinsulinemic hypoglycemia, Hum Mutat, 30 (2009) 1512-1526.
[4] K. Hussain, Mutations in pancreatic ss-cell Glucokinase as a cause of hyperinsulinaemic hypoglycaemia and neonatal diabetes mellitus, Rev Endocr Metab Disord, 11 (2010) 179-183.
[5] A.J. Chakera, A.M. Steele, A.L. Gloyn, M.H. Shepherd, B. Shields, S. Ellard, A.T. Hattersley, Recognition and Management of Individuals With Hyperglycemia Because of a Heterozygous Glucokinase Mutation, Diabetes Care, 38 (2015) 1383-1392.
[6] K. Kamata, M. Mitsuya, T. Nishimura, J. Eiki, Y. Nagata, Structural basis for allosteric regulation of the monomeric allosteric enzyme human glucokinase, Structure, 12 (2004) 429-438.
[7] M. Larion, R.K. Salinas, L. Bruschweiler-Li, B.G. Miller, R. Bruschweiler, Order-disorder transitions govern kinetic cooperativity and allostery of monomeric human glucokinase, PLoS Biol, 10 (2012) e1001452.

[8] E. Van Schaftingen, M. Detheux, M. Veiga da Cunha, Short-term control of glucokinase activity: role of a regulatory protein, Faseb j, 8 (1994) 414-419.
[9] L. Agius, Glucokinase and molecular aspects of liver glycogen metabolism, Biochem J, 414 (2008) 1-18.
[10] M. Veiga-da-Cunha, E. Van Schaftingen, Identification of fructose 6-phosphate- and fructose 1-phosphate-binding residues in the regulatory protein of glucokinase, J Biol Chem, 277 (2002) 8466-8473.
[11] T. Beck, B.G. Miller, Structural basis for regulation of human glucokinase by glucokinase regulatory protein, Biochemistry, 52 (2013) 6232-6239.
[12] M. Veiga-da-Cunha, S. Courtois, A. Michel, E. Gosselain, E. Van Schaftingen, Amino acid conservation in animal glucokinases. Identification of residues implicated in the interaction with the regulatory protein, J Biol Chem, 271 (1996) 6292-6297.
[13] V.V. Heredia, T.J. Carlson, E. Garcia, S. Sun, Biochemical basis of glucokinase activation and the regulation by glucokinase regulatory protein in naturally occurring mutations, J Biol Chem, 281 (2006) 40201-40207.
[14] B. Zelent, S. Odili, C. Buettger, D.K. Zelent, P. Chen, D. Fenner, J. Bass, C. Stanley, M. Laberge, J.M. Vanderkooi, R. Sarabu, J. Grimsby, F.M. Matschinsky, Mutational analysis of allosteric activation and inhibition of glucokinase, Biochem J, 440 (2011) 203-215.
[15] J.M. Choi, M.H. Seo, H.H. Kyeong, E. Kim, H.S. Kim, Molecular basis for the role of glucokinase regulatory protein as the allosteric switch for glucokinase, Proc Natl Acad Sci U S A, 110 (2013) 10171-10176.
[16] J. Grimsby, J.W. Coffey, M.T. Dvorozniak, J. Magram, G. Li, F.M. Matschinsky, C. Shiota, S. Kaur, M.A. Magnuson, J.F. Grippo, Characterization of glucokinase regulatory protein-deficient mice, J Biol Chem, 275 (2000) 7826-7831.
[17] C. Shiota, J. Coffey, J. Grimsby, J.F. Grippo, M.A. Magnuson, Nuclear import of hepatic glucokinase depends upon glucokinase regulatory protein, whereas export is due to a nuclear export signal sequence in glucokinase, J Biol Chem, 274 (1999) 37125-37130.
[18] M.T. Kaminski, J. Schultz, R. Waterstradt, M. Tiedge, S. Lenzen, S. Baltrusch, Glucose-induced dissociation of glucokinase from its regulatory protein in the nucleus of hepatocytes prior to nuclear export, Biochim Biophys Acta, 1843 (2014) 554-564.
[19] L. Agius, Hormonal and Metabolite Regulation of Hepatic Glucokinase, Annu Rev Nutr, 36 (2016) 389-415.
[20] F.M. Matschinsky, B. Zelent, N. Doliba, C. Li, J.M. Vanderkooi, A. Naji, R. Sarabu, J. Grimsby, Glucokinase activators for diabetes therapy: May 2010 status report, Diabetes care, 34 Suppl 2 (2011) S236-243.
[21] F.M. Matschinsky, GKAs for diabetes therapy: why no clinically useful drug after two decades of trying?, Trends Pharmacol Sci, 34 (2013) 90-99.
[22] P. Froguel, H. Zouali, N. Vionnet, G. Velho, M. Vaxillaire, F. Sun, S. Lesage, M. Stoffel, J. Takeda, P. Passa, et al., Familial hyperglycemia due to mutations in glucokinase. Definition of a subtype of diabetes mellitus, N Engl J Med, 328 (1993) 697-702.
[23] F. Ziemssen, C. Bellanne-Chantelot, M. Osterhoff, H. Schatz, A.F. Pfeiffer, To: Lindner T, Cockburn BN, Bell GI (1999). Molecular genetics of MODY in Germany. Diabetologia 42: 121-123, Diabetologia, 45 (2002) 286-287; author reply 287-288.
[24] J. Weng, M. Ekelund, M. Lehto, H. Li, G. Ekberg, A. Frid, A. Aberg, L.C. Groop, K. Berntorp, Screening for MODY mutations, GAD antibodies, and type 1 diabetes--associated HLA genotypes in women with gestational diabetes mellitus, Diabetes care, 25 (2002) 68-71.
[25] C.M. Garcia-Herrero, M. Galan, O. Vincent, B. Flandez, M. Gargallo, E. Delgado-Alvarez, E. Blazquez, M.A. Navas, Functional analysis of human glucokinase gene mutations causing MODY2: exploring the regulatory mechanisms of glucokinase activity, Diabetologia, 50 (2007) 325-333.

[26] J. Oriola, F. Moreno, A. Gutierrez-Nogues, S. Leon, C.M. Garcia-Herrero, O. Vincent, M.A. Navas, Lack of glibenclamide response in a case of permanent neonatal diabetes caused by incomplete inactivation of glucokinase, JIMD Rep, 20 (2015) 21-26.
[27] M. Galan, O. Vincent, I. Roncero, S. Azriel, P. Boix-Pallares, E. Delgado-Alvarez, F. Diaz-Cadorniga, E. Blazquez, M.A. Navas, Effects of novel maturity-onset diabetes of the young (MODY)-associated mutations on glucokinase activity and protein stability, Biochem J, 393 (2006) 389-396.
[28] K.J. Brocklehurst, R.A. Davies, L. Agius, Differences in regulatory properties between human and rat glucokinase regulatory protein, Biochem J, 378 (2004) 693-697.
[29] C. Munoz-Fontela, M. Collado, E. Rodriguez, M.A. Garcia, A. Alvarez-Barrientos, J. Arroyo, C. Nombela, C. Rivas, Identification of a nuclear export signal in the KSHV latent protein LANA2 mediating its export from the nucleus, Experimental cell research, 311 (2005) 96-105.
[30] C.M. Garcia-Herrero, O. Rubio-Cabezas, S. Azriel, A. Gutierrez-Nogues, A. Aragones, O. Vincent, A. Campos-Barros, J. Argente, M.A. Navas, Functional characterization of MODY2 mutations highlights the importance of the fine-tuning of glucokinase and its role in glucose sensing, PLoS One, 7 (2012) e30518.
[31] E.A. Davis, A. Cuesta-Munoz, M. Raoul, C. Buettger, I. Sweet, M. Moates, M.A. Magnuson, F.M. Matschinsky, Mutants of glucokinase cause hypoglycaemia- and hyperglycaemia syndromes and their analysis illuminates fundamental quantitative concepts of glucose homeostasis, Diabetologia, 42 (1999) 1175-1186.
[32] S. Langer, C. Platz, R. Waterstradt, S. Baltrusch, Characterization of two MODY2 mutations with different susceptibility to activation, Biochem Biophys Res Commun, 464 (2015) 1113-1119.
[33] M. Gidh-Jain, J. Takeda, L.Z. Xu, A.J. Lange, N. Vionnet, M. Stoffel, P. Froguel, G. Velho, F. Sun, D. Cohen, et al., Glucokinase mutations associated with non-insulin-dependent (type 2) diabetes mellitus have decreased enzymatic activity: implications for structure/function relationships, Proc Natl Acad Sci U S A, 90 (1993) 1932-1936.
[34] P. Kesavan, L. Wang, E. Davis, A. Cuesta, I. Sweet, K. Niswender, M.A. Magnuson, F.M. Matschinsky, Structural instability of mutant beta-cell glucokinase: implications for the molecular pathogenesis of maturity-onset diabetes of the young (type-2), Biochem J, 322 (Pt 1) (1997) 57-63.
[35] C.V. Burke, C.W. Buettger, E.A. Davis, S.J. McClane, F.M. Matschinsky, S.E. Raper, Cell-biological assessment of human glucokinase mutants causing maturity-onset diabetes of the young type 2 (MODY-2) or glucokinase-linked hyperinsulinaemia (GK-HI), The Biochemical journal, 342 (Pt 2) (1999) 345-352.
[36] M. Capuano, C.M. Garcia-Herrero, N. Tinto, C. Carluccio, V. Capobianco, I. Coto, A. Cola, D. Iafusco, A. Franzese, A. Zagari, M.A. Navas, L. Sacchetti, Glucokinase (GCK) mutations and their characterization in MODY2 children of southern Italy, PLoS One, 7 (2012) e38906.
[37] Gloyn AL, Odili S, Buettger C, Njolstad PR, Shiota C, Magnuson M, M. F., Glucokinase and the regulation of blood sugar: a mathematical model predicts the threshold for glucose stimulated insulin release for GCK gene mutations that cause hyper- and hypoglycaemia., in: Magnuson M, Matschinsky F (Eds.) Glucokinase and glycemic diseases: from the basics to novel therapeutics, Karger, Place Published, 2004, pp. 92-109.
[38] A. Cook, F. Bono, M. Jinek, E. Conti, Structural biology of nucleocytoplasmic transport, Annu Rev Biochem, 76 (2007) 647-671.
[39] B.B. Johansson, K. Fjeld, M.H. Solheim, J. Shirakawa, E. Zhang, M. Keindl, J. Hu, A. Lindqvist, A. Doskeland, G. Mellgren, T. Flatmark, P.R. Njolstad, R.N. Kulkarni, N. Wierup, I. Aukrust, L. Bjorkhaug, Nuclear import of glucokinase in pancreatic beta-cells is mediated by a nuclear localization signal and modulated by SUMOylation, Mol Cell Endocrinol, (2017).

[40] S. Baltrusch, F. Francini, S. Lenzen, M. Tiedge, Interaction of glucokinase with the liver regulatory protein is conferred by leucine-asparagine motifs of the enzyme, Diabetes, 54 (2005) 2829-2837.
[41] A.K. Casey, B.G. Miller, Kinetic Basis of Carbohydrate-Mediated Inhibition of Human Glucokinase by the Glucokinase Regulatory Protein, Biochemistry, 55 (2016) 2899-2902.
[42] U. Kutay, S. Guttinger, Leucine-rich nuclear-export signals: born to be weak, Trends Cell Biol, 15 (2005) 121-124.
[43] S. Kosugi, M. Hasebe, M. Tomita, H. Yanagawa, Nuclear export signal consensus sequences defined using a localization-based yeast selection system, Traffic, 9 (2008) 2053-2062.
[44] T. Guttler, T. Madl, P. Neumann, D. Deichsel, L. Corsini, T. Monecke, R. Ficner, M. Sattler, D. Gorlich, NES consensus redefined by structures of PKI-type and Rev-type nuclear export signals bound to CRM1, Nat Struct Mol Biol, 17 (2010) 1367-1376.
[45] H.Y. Fung, S.C. Fu, Y.M. Chook, Nuclear export receptor CRM1 recognizes diverse conformations in nuclear export signals, Elife, 6 (2017).
[46] D. Xu, A. Farmer, G. Collett, N.V. Grishin, Y.M. Chook, Sequence and structural analyses of nuclear export signals in the NESdb database, Mol Biol Cell, 23 (2012) 3677-3693.
[47] D. Engelsma, R. Bernad, J. Calafat, M. Fornerod, Supraphysiological nuclear export signals bind CRM1 independently of RanGTP and arrest at Nup358, Embo j, 23 (2004) 3643-3652.
[48] T. la Cour, L. Kiemer, A. Molgaard, R. Gupta, K. Skriver, S. Brunak, Analysis and prediction of leucine-rich nuclear export signals, Protein Eng Des Sel, 17 (2004) 527-536.
[49] A. Raimondo, A.J. Chakera, S.K. Thomsen, K. Colclough, A. Barrett, E. De Franco, A. Chatelas, H. Demirbilek, T. Akcay, H. Alawneh, N.D.M.C. International, S.E. Flanagan, M. Van De Bunt, A.T. Hattersley, A.L. Gloyn, S. Ellard, N.D.M.C. International, Phenotypic severity of homozygous GCK mutations causing neonatal or childhood-onset diabetes is primarily mediated through effects on protein stability, Human molecular genetics, 23 (2014) 6432-6440.
[50] J.A. Pfefferkorn, Strategies for the design of hepatoselective glucokinase activators to treat type 2 diabetes, Expert Opin Drug Discov, 8 (2013) 319-330.
[51] D.J. Lloyd, D.J. St Jean, Jr., R.J. Kurzeja, R.C. Wahl, K. Michelsen, R. Cupples, M. Chen, J. Wu, G. Sivits, J. Helmering, R. Komorowski, K.S. Ashton, L.D. Pennington, C. Fotsch, M. Vazir, K. Chen, S. Chmait, J. Zhang, L. Liu, M.H. Norman, K.L. Andrews, M.D. Bartberger, G. Van, E.J. Galbreath, S.L. Vonderfecht, M. Wang, S.R. Jordan, M.M. Veniant, C. Hale, Antidiabetic effects of glucokinase regulatory protein small-molecule disruptors, Nature, 504 (2013) 437-440.
[52] C. Hale, D.J. Lloyd, A. Pellacani, M.M. Veniant, Molecular targeting of the GK-GKRP pathway in diabetes, Expert Opin Ther Targets, 19 (2015) 129-139.

Figure Legends

Figure 1. *Effect of temperature on the stability of the GST-GCK mutants.* Stock enzyme solutions were diluted to 250 μg/ml in storage buffer as described in Supplementary Material and Methods. **A**, Enzyme solutions were incubated for 30 min at different temperatures and then assayed at 30 ºC. **B**, Enzyme solutions were incubated for different periods of time at 50ºC. 100% activity corresponds to a specific activity (U/mg of protein) of 23.4 ±1.6; 5.8 ±0.7; 1.6 ±0.2 and 4.9±1.3 for GST-GCK, GST-GCK(V302E), GST-GCK(L304P) and GST-GCK(L309H), respectively. *Circle*, GST-GCK; *square*, GCK(V302E); *triangle*, GST-GCK(L304P); *rhombus*, GST-GCK(L309H). Data represent means ± SD of at least 4 measurements from 2 independent protein purifications.

Figure 2. *Inhibition of wild type and mutant GCK activity by GKRP.* Enzyme activity was measured at a GST-GCK wild type or mutant concentration of 61 nmol/l in the presence of the indicated amount of purified Flag-GKRP. 100% activity corresponds to a specific activity (U/mg of protein) of 4.6±0.1; 0.65 ±0.17; 1.16 ±0.2; 0.23 ±0.04; 0.58 ±0.09 and 0.73 ±0.19 for GST-GCK, GST-GCK(V302E), GST-GCK(R303W), GST-GCK(L304P), GST-GCK(R308W) and GST-GCK(L309H), respectively. *Solid circle*, GST-GCK; *solid square*, GCK(V302E); *solid triangle*, GST-GCK(R303W); *solid rhombus*, GST-GCK(L304P); *open circle* GST-GCK(R308W); *open square*, GST-GCK(L309H); *open triangle*, GST-GCK(A456V). Data represent means ± SD for 4 assays using at least 2 independent enzyme purifications.

Figure 3. *Subcellular localization of GFP-GCK variants and GKRP-mCherry on transient cotransfection into HepG2 cells*. **A, B** Representative fluorescence images of HepG2 cotransfected cells. **A** Coexpression of wild type GFP-GCK (WT) with mCherry or GKRP-mCherry . **B** Coexpression of GFP-GCK mutants with GKRP-mCherry. GFP, mCherry and DAPI fluorescence channels are shown. Scale bar 10 μm. **C** Percentage of cells with GFP nuclear enrichment. Data, extracted from Supplementary Table 2, represent means ± SD of at least 100 cells visualised in, at least, 3 independent transfections (n≥300). Data shown for mutations E300Q and L309H correspond to only one transfection (n= 161 and 127 cells, respectively, Supplementary Table S2). (*) $p<0.001$ versus cells cotransfected with wild type GFP-GCK and GKRP-mCherry.

Figure 4. *Two-hybrid interaction of Gal4-binding domain (GBD)–GRKP with Gal4-activating domain (GAD)–GCK.* β-galactosidase filter lift assay is shown for at least 7 independent transformants.

Figure 5. *Schematic representation of the GCK$^{(299-359)}$-GFP fusion protein and comparison of the GCK-NES sequence with the NES consensus.* **A** GCK$^{(299-359)}$-GFP construct designed by [14] showing rat GCK-NES and mt3 mutant sequences. **B** MODY2 mutant GCK-NES sequences. **C** alignment of the NES consensus class 1b and human GCK-NES. ϕ, hydrophobic residue; X, any residue. Numbers indicate position of residues in GCK protein sequence.

Figure 6.- *Subcellular localization of GFP and wild type or mutant GCK$^{(299-359)}$-GFP on transient transfection into HEK293T cells*. HEK293T cells were transfected with plasmid pEGFP-N2-ratGCK$^{(299-359)}$ or mutant derivatives. **A,B** Representative GFP and DAPI confocal images of transfected cells are shown. Scale bar 10 μm. **C** Percentage of cells with GFP or *GCK$^{(299-359)}$-GFP* fluorescence accumulated in the nucleus. Data, extracted from Supplementary Table S3, are shown as means ± SD of at least 100 cells visualised in, at least, 3 independent transfections (n≥300). **D** Nuclear to cytoplasmic GFP fluorescence intensity ratio (N/C ratio). K308W in rat GCK$^{(299-359)}$-GFP corresponds to MODY2 mutation R308W. Data are means ± SD of at least three independent experiments with a total of 10-24 cell images analysed. (*) $p<0.05$ versus cells transfected with wild type GCK$^{(299-359)}$-GFP (WT).

Figure 7.- *Effect of CRM1 overexpression on the subcellular localization of GFP and wild type or mutant GCK$^{(299-359)}$-GFP on transiently transfected HEK293T cells*. HEK293T cells were cotransfected with plasmid pEGFP-N2-ratGCK$^{(299-359)}$ or mutant derivatives andpCMV-HA-CRM1, and processed for immunofluorescence. HA-tagged CRM1 was revealed with *monoclonal rat anti-HA Tag* and *goat anti rat IgG (H&L):Texas-Red* antibodies. K308W in rat GCK$^{(299-359)}$-GFP corresponds to MODY2 mutation R308W. **A,B** Representative GFP, Texas-Red and DAPI confocal images of transfected cells are shown. Scale bar 10 μm. **C** Percentage of cells with GFP or GCK$^{(299-359)}$-GFP fluorescence accumulated in the nucleus. Data, extracted from Supplementary Table S5, are shown as means ± SD of about 100 cells visualised in 3 independent transfections (n≥290). **D** Nuclear to cytoplasmic GFP fluorescence intensity ratio (N/C ratio). Data are means ± SD of 3

independent experiments with a total of 12-20 cell images analysed. (*) $p<0.05$ versus cells cotransfected with HA-CRM1 and wild type $GCK^{(299-359)}$-GFP (WT).

Figure 8.- *Localization of mutations in the structural model of human glucokinase.* E300 is shown in green, V302 in yellow, R303 in blue, L304 in magenta, L306 in pink, R308 in cyan and L309 in orange. **A** Location of mutated residues in the closed conformation of GCK (1V4S) [6]. **B** Hydrophobic positions Φ at the GCK-NES sequence are shown. Same colour assignment shown in b apply for a and c. **C** Location of mutated residues in the open conformation of GCK bound to GKRP (4LC9) [11]. **D** to **G** An enlargement of the region of interest in the closed conformation of GCK is shown in each panel. Left panels represent the wild-type state while right panels show the predicted collisions (red discs) of substituted residues to surrounding aminoacids (shown in black). GCK conformations are represented using the Pymol Molecular Graphics System (Schrödinger).

Table 1.- Kinetic parameters of wild-type and MODY2 mutant GST-GCK fusion proteins.

Protein	Protein yield (mg/l)	Kcat (s^{-1})	$S_{0.5}$ for glucose (mmol/l)	h	Km for ATP (mmol/l)	RAI
GST-GCK (n=24)	5.19 ± 3.90 (14)	55.30 ± 14.40	7.69 ± 0.43	1.45 ± 0.06	0.52 ± 0.06	1.00 ± 0.3
GST-GCK(V302E) (n=7)	1.75 ± 0.40*(3)	7.73 ± 4.67*	10.17 ± 0.89*	1.32 ± 0.10*	0.65 ± 0.01*	0.13 ± 0.08*
GST-GCK(L304P) (n=7)	1.61 ± 0.64*(5)	7.38 ± 2.24*	11.30 ± 1.02*	1.05 ± 0.18*	0.59 ± 0.06*	0.17 ± 0.04*
GST-GCK(L306R) (n=7)	1.07 ± 0.13*(3)	0.70 ± 0.25*	11.40 ± 1.90*	0.99 ± 0.05*	0.40 ± 0.01*	0.03 ± 0.01*
GST-GCK(L309H) (n=6)	5.16 ± 0.1 (3)	9.56 ± 3.00*	9.98 ± 0.97*	1.37 ± 0.15	0.45 ± 0.07*	0.15 ± 0.08*

Data are shown as mean ± SD for n measurements. In protein yield column, parenthesis indicates the number of separate enzyme preparations for wild-type and mutant GST-GCK. The Hill coefficient (h) and the relative activity index (RAI) are unit-less. (*) $p<0.05$

Highlights

The glucokinase α8-helix is important for enzyme stability and kinetics

MODY2 mutations L306R and L309P prevent GKRP-mediated nuclear import of glucokinase

The MODY2 mutation L304P inactivates the glucokinase nuclear export signal

The function of the glucokinase nuclear export signal depends on exportin 1

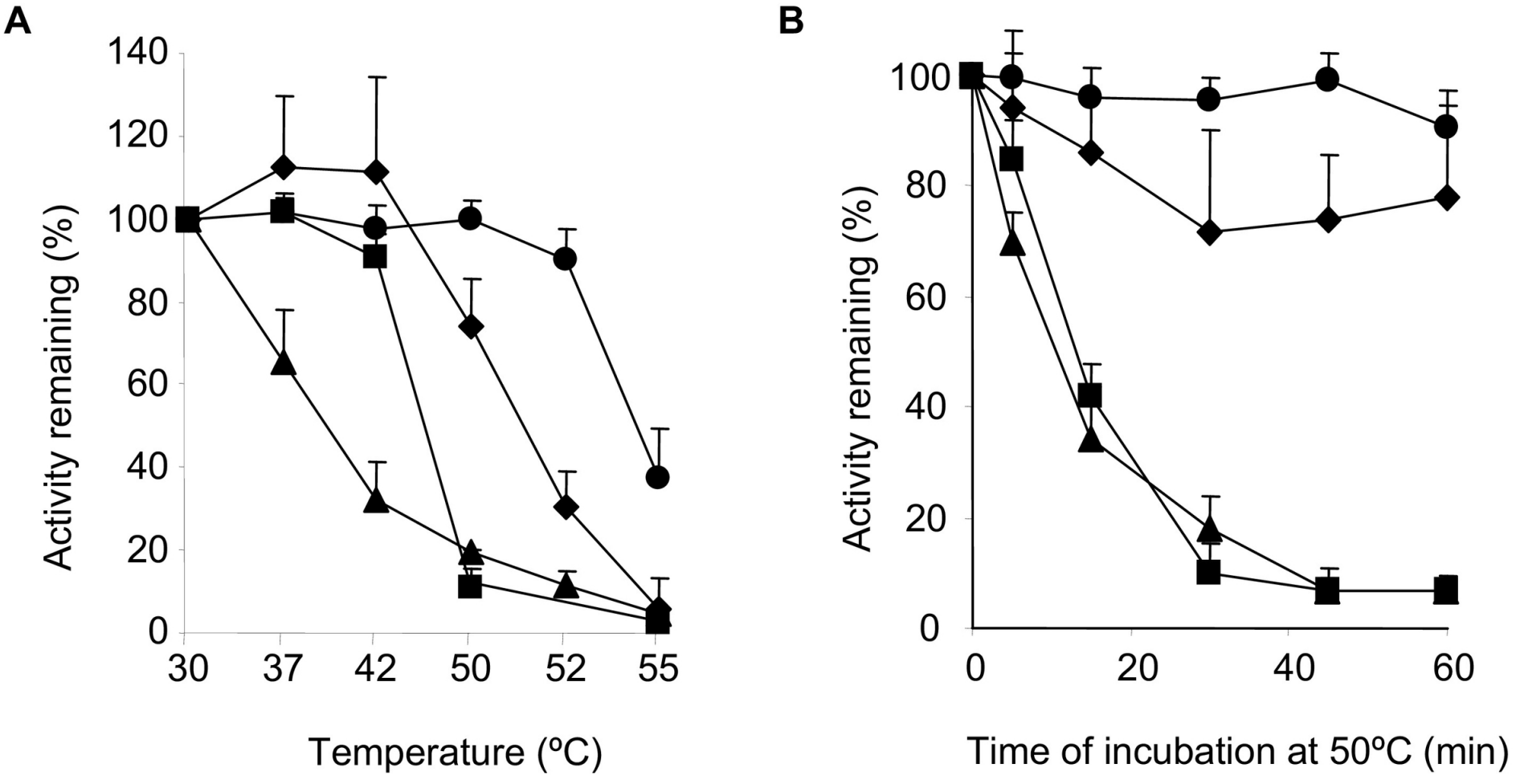
A
140
120
100
80
60
40
20
0
Activity remaining (%)
30
37
42
50
52
55
Temperature (ºC)
B
100
80
60
40
20
0
Activity remaining (%)
0
20
40
60
Time of incubation at 50ºC (min)

Figure 1

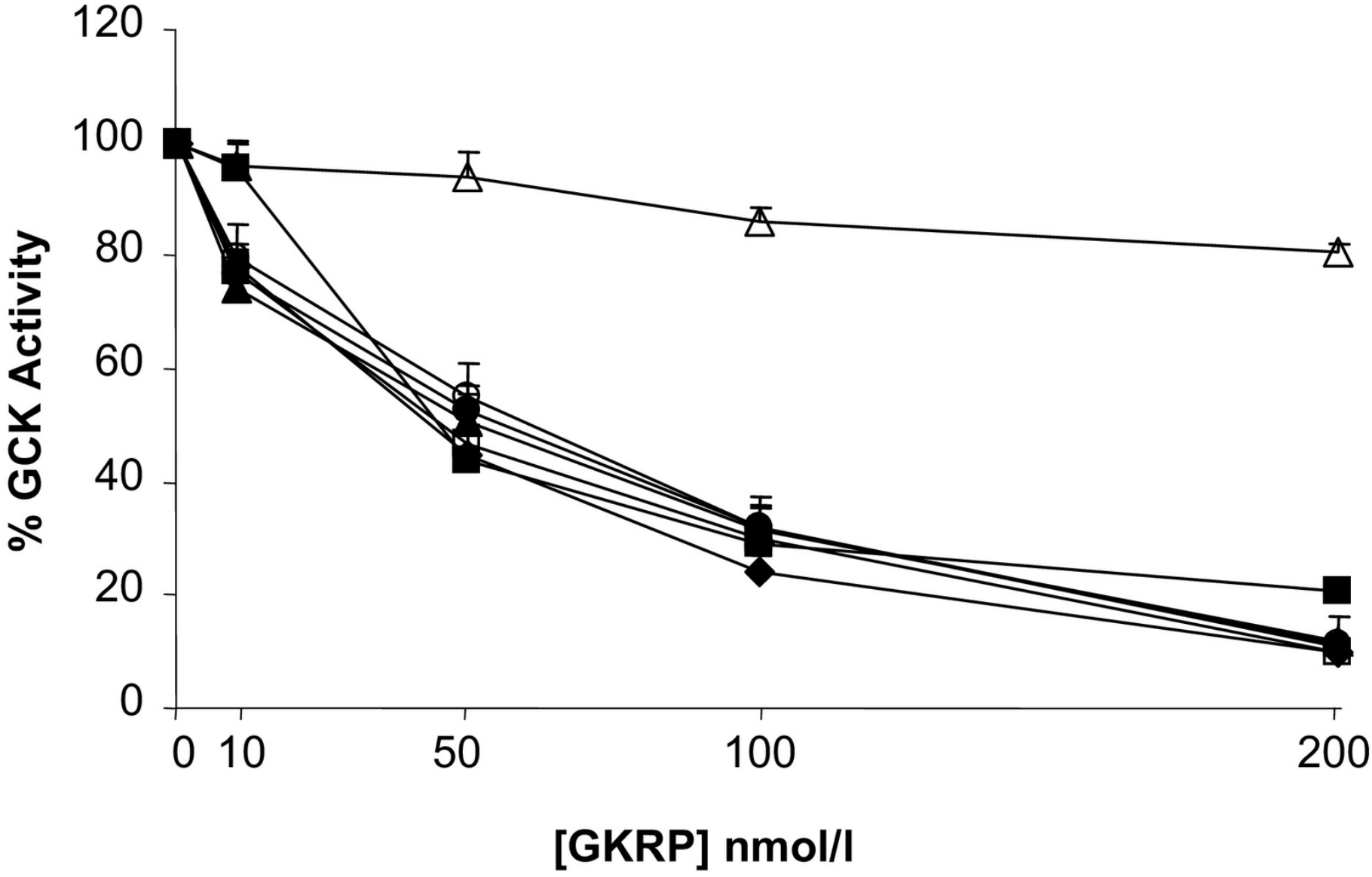

Figure 2

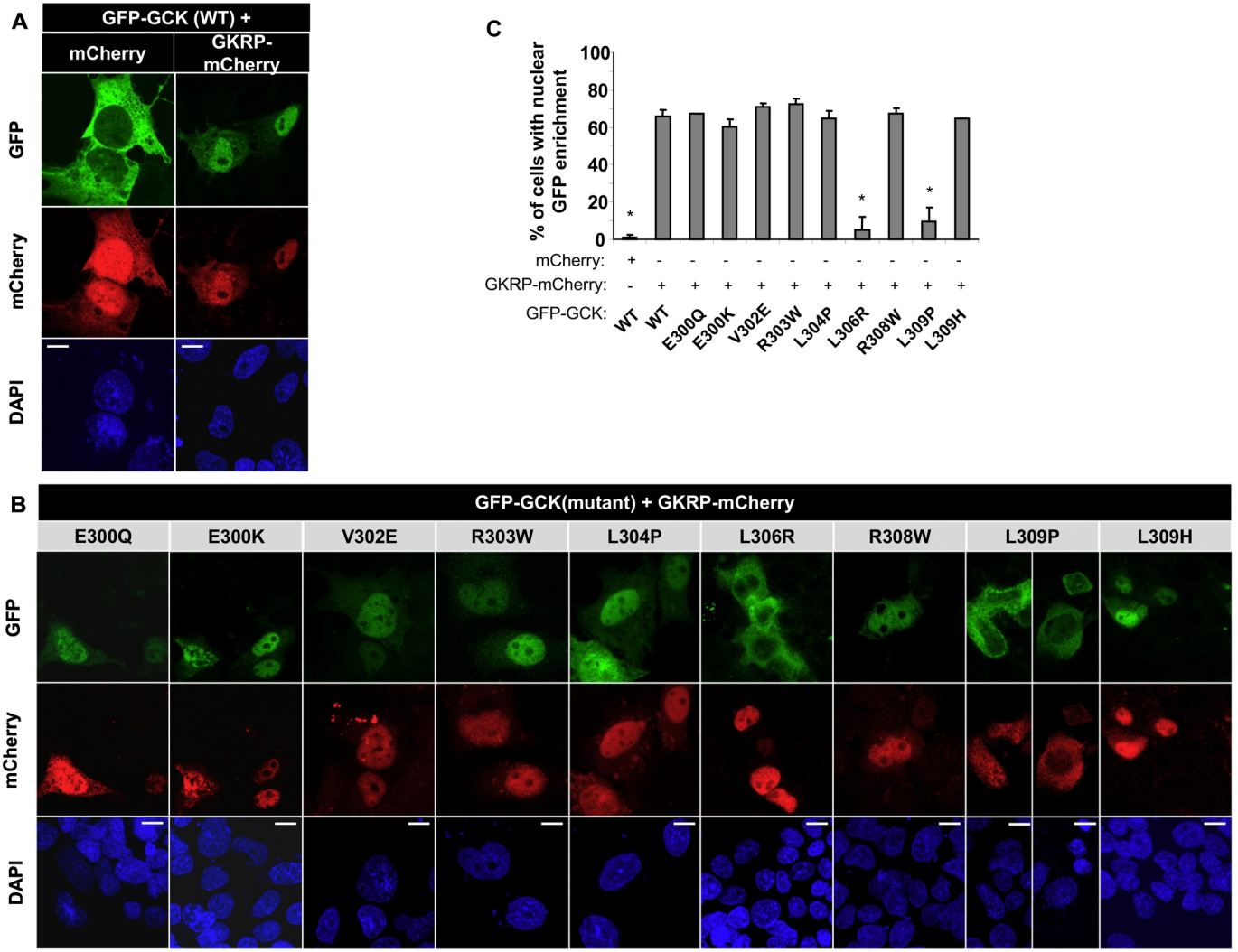
A
GFP-GCK (WT) +
mCherry
GKRP-mCherry
GFP
mCherry
DAPI
C
% of cells with nuclear GFP enrichment
100
80
60
40
20
0
mCherry:
GKRP-mCherry:
GFP-GCK:
WT
WT
E300Q
E300K
V302E
R303W
L304P
L306R
R308W
L309P
L309H
B
GFP-GCK(mutant) + GKRP-mCherry
E300Q
E300K
V302E
R303W
L304P
L306R
R308W
L309P
L309H
GFP
mCherry
DAPI

Figure 3

GBD-fusion	GAD-fusion
GKRP	GCK
GKRP	GCK(V302E)
GKRP	GCK(L304P)
GKRP	GCK(L306R)
GKRP	GCK(R308W)
GKRP	GCK(L309P)
GKRP	GCK(L309H)

Two-hybrid interaction (β-galactosidase filter lift assay) for independent transformants

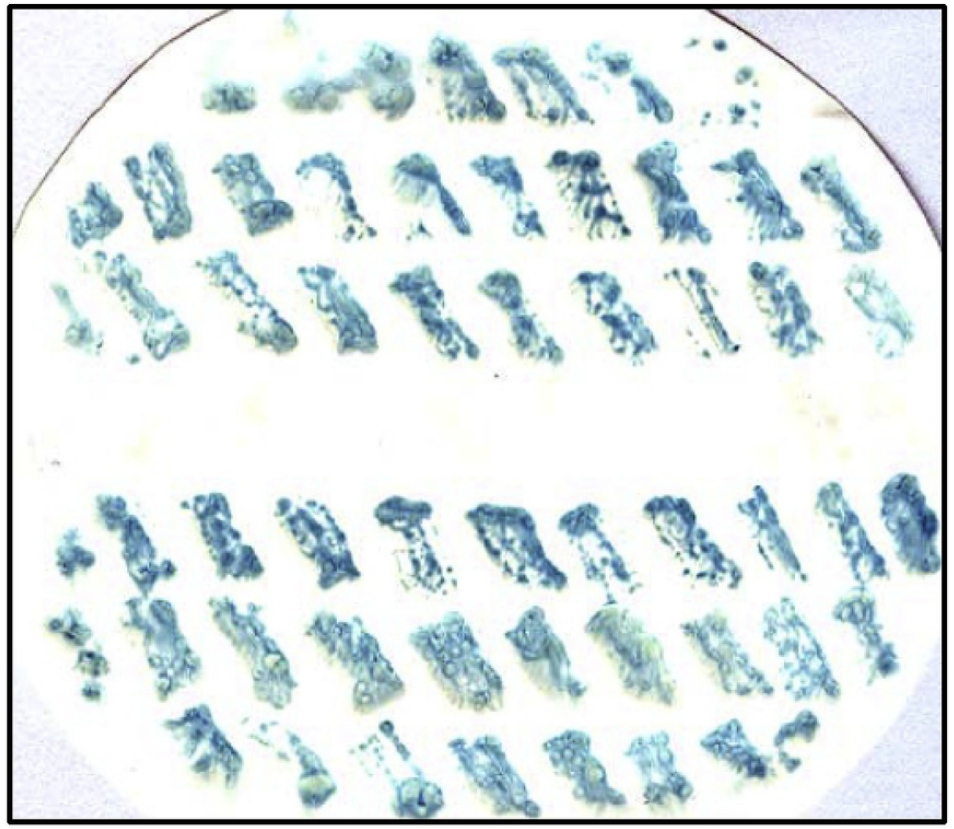

Figure 4

A

^{300}ELVRLVLLKLV^{310} rat GCK-NES sequence

^{300}ELVRLV**AA**K**A**V^{310} mt3 (inactive GCK-NES)

B

^{300}**Q**LVRLVLLKLV^{310} GCK-NES (E300Q)

^{300}**K**LVRLVLLKLV^{310} GCK-NES (E300K)

^{300}EL**E**RLVLLKLV^{310} GCK-NES (V302E)

^{300}ELV**W**LVLLKLV^{310} GCK-NES (R303W)

^{300}ELVR**P**VLLKLV^{310} GCK-NES (L304P)

^{300}ELVRLV**R**LKLV^{310} GCK-NES (L306R)

^{300}ELVRLVLL**W**LV^{310} GCK-NES (K308W)

^{300}ELVRLVLLK**P**V^{310} GCK-NES (L309P)

^{300}ELVRLVLLK**H**V^{310} GCK-NES (L309H)

C

ϕ_1XXϕ_2XXϕ_3Xϕ_4 NES consensus Class 1b

^{300}**ELVRLVLLRLV**^{310} human GCK-NES sequence

Figure 5

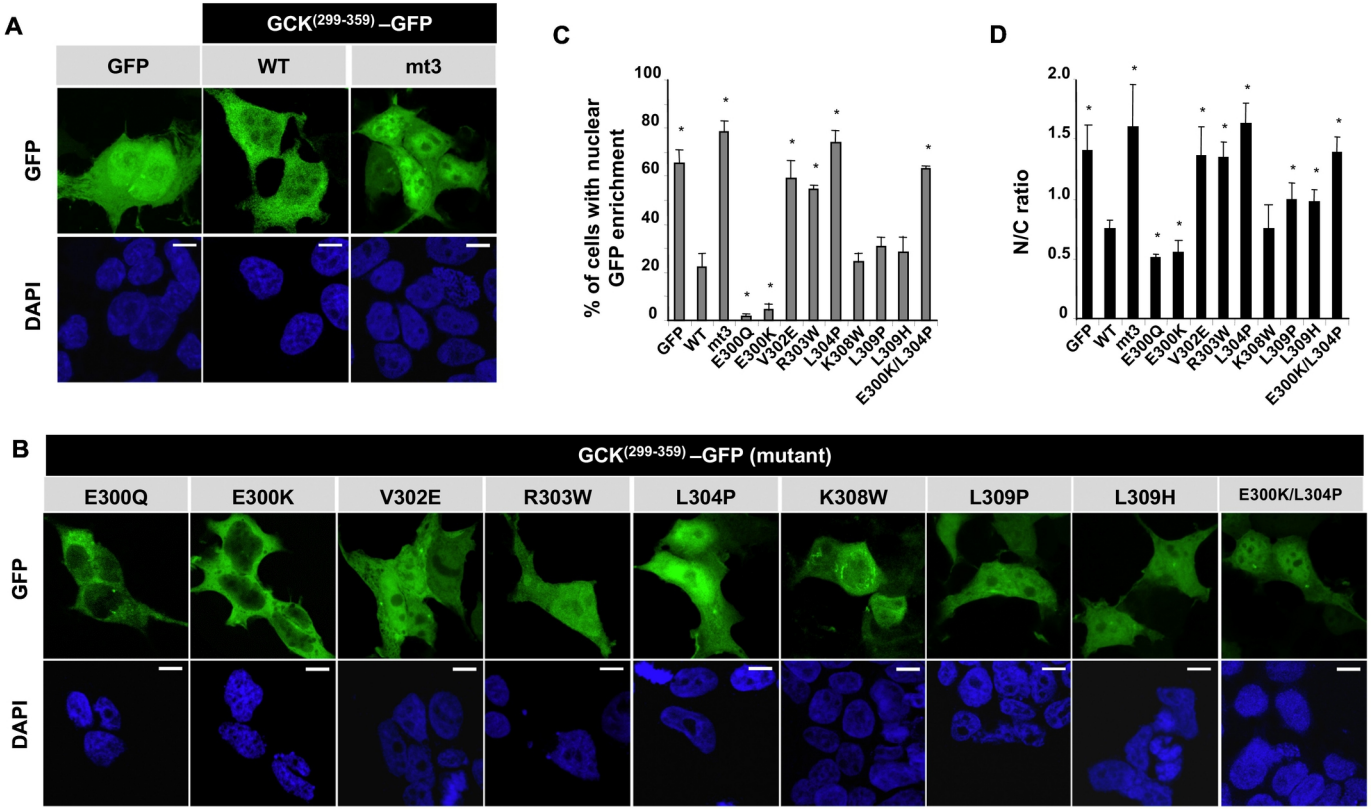
A
GCK(299-359) –GFP
GFP
WT
mt3
GFP
DAPI
C
% of cells with nuclear GFP enrichment
100
80
60
40
20
0
GFP
WT
mt3
E300Q
E300K
V302E
R303W
L304P
K308W
L309P
L309H
E300K/L304P
D
N/C ratio
2.0
1.5
1.0
0.5
0
B
GCK(299-359) –GFP (mutant)
E300Q
E300K
V302E
R303W
L304P
K308W
L309P
L309H
E300K/L304P
GFP
DAPI

Figure 6

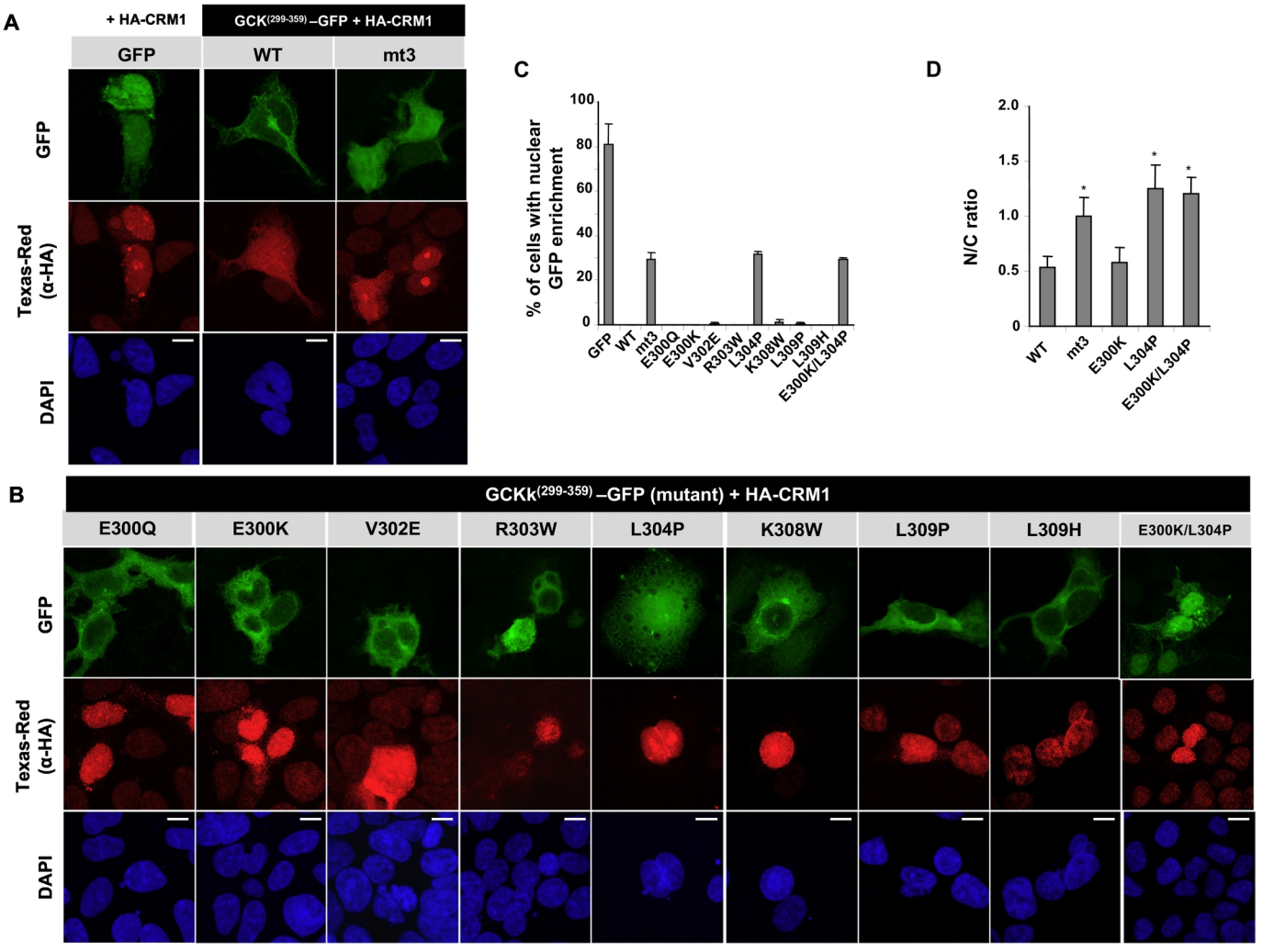
A
+ HA-CRM1
GCK(299-359)–GFP + HA-CRM1
GFP
WT
mt3
GFP
Texas-Red (α-HA)
DAPI
C
% of cells with nuclear GFP enrichment
100
80
60
40
20
0
GFP
WT
mt3
E300Q
E300K
V302E
R303W
L304P
K308W
L309P
L309H
E300K/L304P
D
N/C ratio
2.0
1.5
1.0
0.5
0
WT
mt3
E300K
L304P
E300K/L304P
B
GCKk(299-359)–GFP (mutant) + HA-CRM1
E300Q
E300K
V302E
R303W
L304P
K308W
L309P
L309H
E300K/L304P
GFP
Texas-Red (α-HA)
DAPI

Figure 7

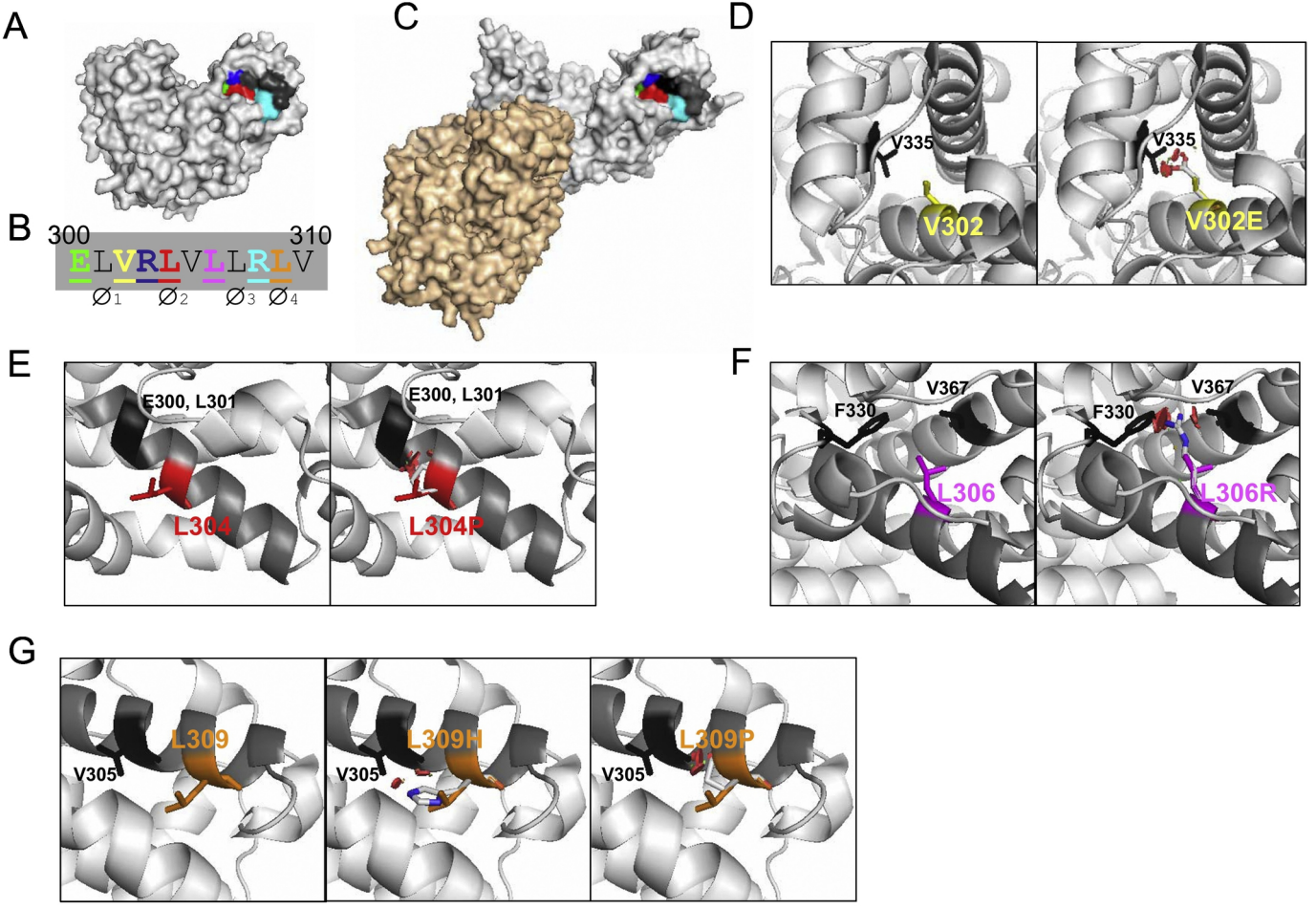
A
B
300
310
ELVRLVLLRLV
∅1 ∅2 ∅3 ∅4
C
D
V335
V302
V335
V302E
E
E300, L301
L304
E300, L301
L304P
F
F330
V367
L306
F330
V367
L306R
G
L309
V305
L309H
V305
L309P
V305

Figure 8